Optik 127 (2016) 7319–7325

Contents lists available at ScienceDirect

Optik

journal homepage: www.elsevier.de/ijleo

Structural, morphological, optical, and electrical properties of In_2O_3 nanostructured thin films

A. Bouhdjer[a], H. Saidi[a], A. Attaf[a,*], M.S. Aida[b], Mohamed JlassI[c], I. Bouhaf[a], Y. Benkhetta[a], H. Bendjedidi[a,b,c]

[a] Physic Laboratory of Thin Films and Applications LPCMA, University of Biskra, Algeria
[b] Laboratoire de Couches Minces et Interfaces Faculté des Sciences Université de Constantine, Algeria
[c] Laboratoire de Photovoltaïque, Centre de Recherche et des Technologies de l'Energie, Technopole de Borj-Cédria, BP 95, 2050 Hammam-Lif, Tunisia

ARTICLE INFO

Article history:
Received 20 December 2015
Received in revised form 24 January 2016
Accepted 10 May 2016

Keywords:
Indium oxide
Flow rate
Ultrasonic spray
Optical and electrical properties

ABSTRACT

Indium oxide (In_2O_3) nanostructured thin films are prepared by ultrasonic spray technique on glass substrates at 350 °C. Solution flow rate influence on the structural, morphological, optical and electrical properties of these samples is then studied. A number of techniques, as well as X-ray diffraction (XRD), SEM, and UV–vis are used to characterize the physical properties of these films. X-ray diffraction analysis indicates the spherical indium oxide nanoparticles (20 nm to 67 nm) were in single-crystalline phase with body-centered cubic structure, and the preferred growth orientation change with the change of Solution Spray Rate. The films exhibit high optical transparency >80% in the visible region. The higher value of the optical band gap was 3.93 eV due to the quantum confinement effect. The film grown at 55 ml/h showed low resistivity (8.5 10^{-3} Ω cm).

1. Introduction

Indium oxide (In_2O_3) is a well-known transparent semiconducting oxide thin film. Due to its high optical transmittance in the visible and near infrared regions. It is frequently used for photovoltaic devices, transparent windows; liquid crystal displays (LCD), light emitting diode (LED), solar cell, gas sensors and anti-reflecting coatings [1]. To date, there are numerous deposition techniques that have been demonstrated to grow In_2O_3 films such as spray pyrolysis [2], vacuum evaporation [3], magnetron sputtering [4], dc-sputtering [5], sol gel [6], pulsed laser ablation [7]. However, the properties of In_2O_3 film depend strongly by the used deposition technique and deposition parameters, In this paper we will focus on the ultrasonic spray technique, as it is simple, flexible, low cost and applicable for large-scale production.

Several published literatures show that the structural and electrical properties of undoped and doped In_2O_3 films were closely related to the preferred grains orientation [8,5]. The crystal grain orientation dependence from the film deposition parameters such as temperature [9], deposition time [10]. In this paper, In_2O_3 thin films were grown on glass substrate using ultrasonic spray technique. We have studied influence of the solution flow rate on the films texture, morphological, optical and electrical properties of these films.

* Corresponding author.
E-mail addresses: ab_attaf@univ-biskra.dz, ab.attaf@gmail.com (A. Attaf).

http://dx.doi.org/10.1016/j.ijleo.2016.05.035
0030-4026/

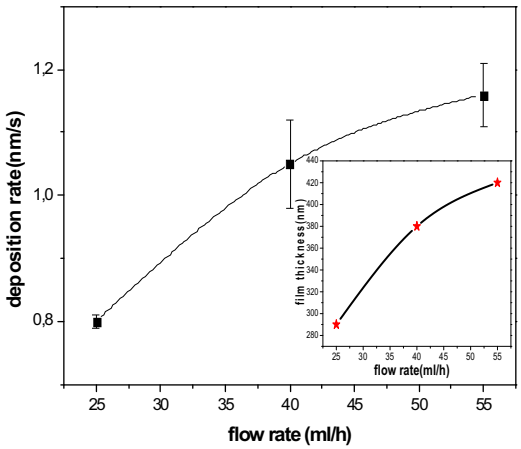

Fig. 1. Variation of deposition rate as a function of solution flow rate, inset shows film thickness.

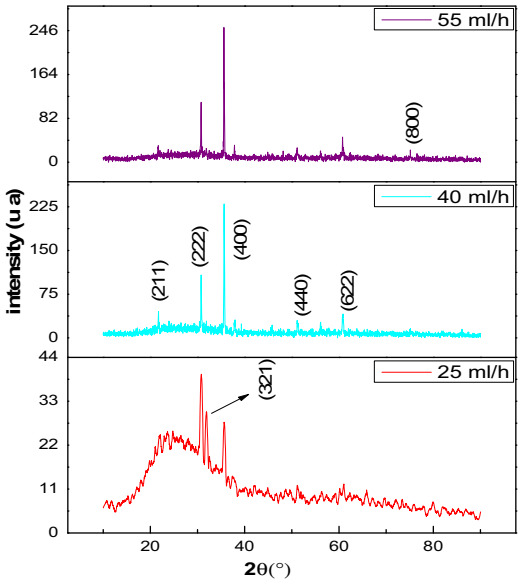

Fig. 2. XRD diffraction pattern of In_2O_3 thin films prepared with different spray rates.

2. Experimental procedure

Indium Oxide thin films were prepared by spraying a solution containing a 0.1 M of indium chloride $InCl_3$ in absolute volume of ethanol as a solvent on glass substrates heated at 350 °C. The glass substrates were chemically cleaned before the deposition. In all deposition the distance spray nozzle–substrate equals 4.5 cm and the deposition time fixed at 6 min. All the parameters were kept constant and only the solution flow rate varied from 25 to 55 ml/h, the later is controlled by (Syringe pump PHOENIX D-CP). The structure and morphology of the films were analyzed by X-ray spectroscopy on a D8 ADVANCE Diffractometer using a Cu Kα radiation (λ = 1.5405 A), JOEL model JSM 6301F a scanning electron microscopy, respectively, the optical transmittance spectra was obtained using UV–vis spectrophotometer, these measurements were performed using glass as reference in a wavelength range of 200–800 nm. The electrical resistivity was determined using the four-point method.

3. Results and discussion

Fig. 1 shows variation in deposition rate (nm/s) with solution flow rate. It remarked that the deposition rate increase with increasing of the solution flow rate. This attributed to the increase of film thickness due to the increase of the sprayed solution volume arriving to substrate surface.

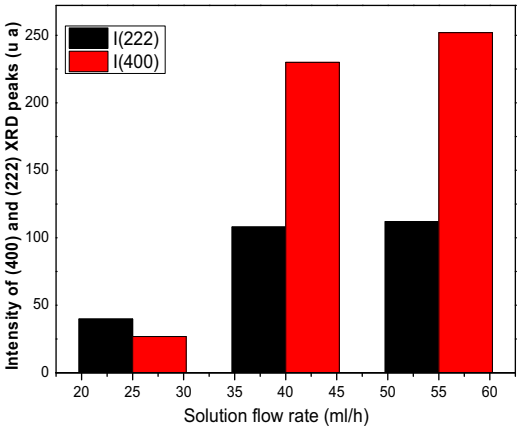

Fig. 3. Solution flow rate effect on the film texture.

Table 1
structural parameters of In_2O_3 films at different solution flow rate.

Flow rate ml/h	Angle (deg)	*hkl*	Crystallite size (nm)	Strain (ε) $\times 10^{-3}$	Dislocationdensity (δ) $\times 10^{14}$ lines/m^2
25	30.69	222	19.8	1.81	25.2
	35.58	400	20.00	1.75	25.0
40	30.68	222	66.39	0.44	2.26
	35.58	400	65.10	0.50	2.35
55	30.70	222	66.70	0.43	2.24
	35.56	400	67.35	0.41	2.20

The XRD spectra of In_2O_3 thin films grown at various solution flow rates are shown in Fig. 2. It can be observed that the In_2O_3 thin films reveal polycrystalline structure with various reflection peaks such as (211),(222), (321), (400), (411), (440) and (622). These peaks, correspond to the body cantered cubic structure of In_2O_3 (JCPDS card no 06-0416). To investigate the dependence of structural properties on solution flow rate, we studied the variation of (222) and (400) diffraction peak intensity (see Fig. 3). On the one hand, the increase in intensity of diffraction peak with increasing solution sprayed indicates the development crystallinity of these films [11]. On the other hand, the film texture change from the [111] direction to [100] direction with the increasing of solution flow rate. This can be attributed to increasing the growth rate, which lead to prevent the incorporation of oxygen in the structure [12], and this will permit to presence the preferred growth of (400) grains [13,14]. The decreasing of the oxygen concentration in the film confirmed by the EDX analysis (included below). This change in the film texture due to the increase of the film thickness is discussed in our earlier work [10]. Thilakan and Kumar presented a similar change in the film texture from (2 2 2) to (4 0 0) with the increase of the deposition rate [15] while H. Seffes et al. reported a (1 1 1)/(2 1 1) texture for sputtered In_2O_3 thin films [16].

The average grains size D of In_2O_3 is estimated using Scherrer's formula [17]:

$$D = \frac{0.9\lambda}{\beta\cos\theta} \tag{1}$$

where θ is the Bragg's angle and β is the full width at half maximum (FWHM) of the peak, λ is the X-ray wavelength.

The strain (ε) values of In_2O_3films are calculated by the following formula [18]:

$$\varepsilon = \frac{\beta\cos\theta}{4} \tag{2}$$

The dislocation density (δ) is calculated using the formula [19]:

$$\delta = \frac{1}{D^2} \tag{3}$$

The grain size, strain and dislocation density of (222) and (400) planes are reported in Table 1. The results show that average grain size increases from 19 to 67 nm with increasing of the solution flow rate. This is probably due to the increased the nucleation density and the average nucleus size due to an increase of the solute atoms arriving to substrate [20,21]. G. Korotcenkov et al. found that the grain size increase with increase of the solution flow rate [22]. However the strain and dislocation density decrease continuously with increasing solution spray rate. This is due to the Improvement of crystalin quality of these films [23].

Fig. 4 shows the SEM surface Images of the In_2O_3 films. For the film deposited at 25 ml/h (Fig. 4.a.), a large number of quasi-pyramidal shaped crystallites are observed. Also, the SEM surface image of this film show distinct grain boundaries. However, the samples deposited at 40 ml/h (Fig. 4. (b)) and 55 ml/h (Fig. 4. (c)) show that the films surface are porous, relatively smooth

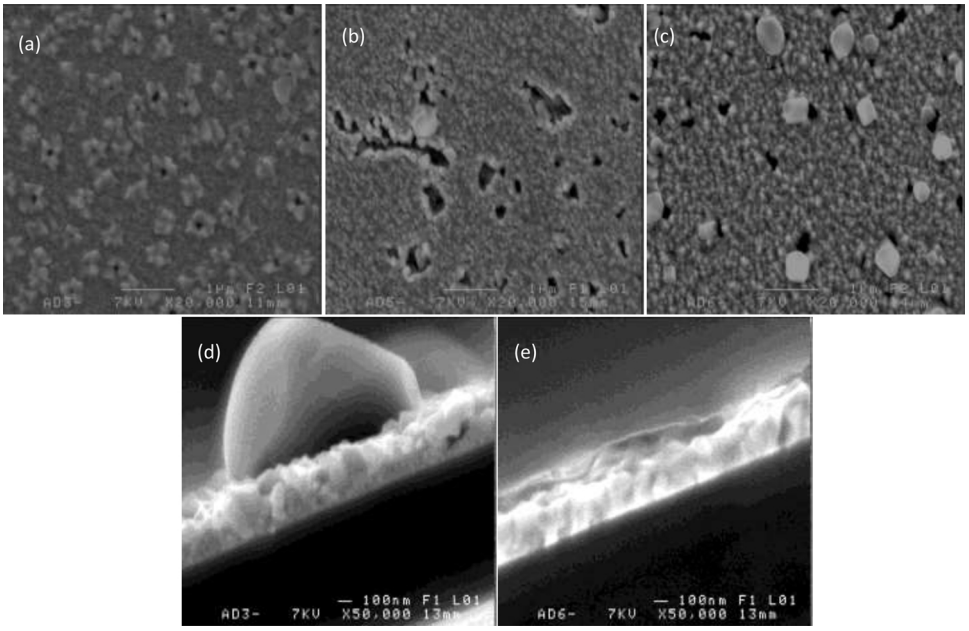

Fig. 4. SEM surface and cross-sectional images of the In_2O_3 thin films deposited at various flow rate of: (a) and (d) 25 ml/h, (b) 40 ml/h, (c) and (e) 55 ml/h.

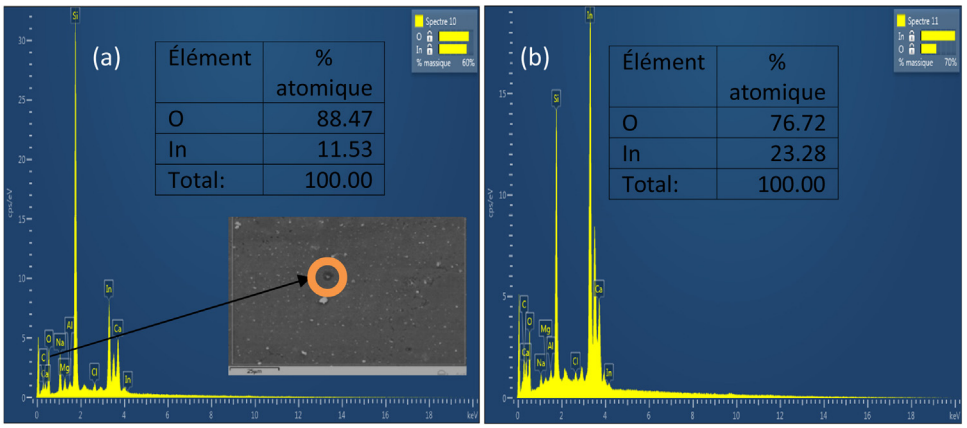

Fig. 5. EDS analysis of the In_2O_3 thin films deposited at various flow rate of: (a) 25 ml/h and (b) 55 ml/h.

and granular without discernible boundaries. On the other hand, figure (4.e) shows that the film deposited at 55 ml/h has approximately columnar structure compared with the film deposited at 25 ml/h (Fig. 4d). This result goes in harmony with our earlier work [10]. The EDX spectrum generated by the incident electron beam were carried out to investigate the composition of indium oxide films formed, It can be observed from Fig. 5 that a clear variation in the concentration of the oxygen and indium with the increase of the solution flow rate. The concentration of the oxygen

decrease from 88.47 at.% to 76.72 at.%, whereas the concentration of the indium increase from 11.53 at.% to 23.28 at.%. These results consistent with the XRD analyses. The presence of the calcium and silicon peak in the spectrum is due to the glass substrate, but the presence of others elements such as carbon may be due to the contamination.

The optical transmission spectrum for In_2O_3 films deposited at various solution flow rate are shown in Fig. 6, the film deposited at 40 ml/h shows maximum visible transmittance (VT) of ~91%, whereas the films deposited at 25 ml/h show lesser transmittance around 81% despite that this film is the thiner. Bu [24] and Bendjedidi et al. [25] have found the similar observation. The low transmittance observed in the thiner layer might be due to the less crystallinity [26] and/or the rough surface of this film [27]. Furthermore, it is clear that the interference fringes absence in the spectrum of films deposited at 25 ml/h and 55 ml/h. This can be attributed to the roughness of the interface air/film; incident light is diffused instead of reflected in one direction [28]. Moreover, the beginning of its presence in the transmission spectrum of the film deposited at 40 ml/h indicates that the film surface is less roughness. This is supported by the SEM surface images which indicate that the film deposited at 40 ml/h is less roughness.

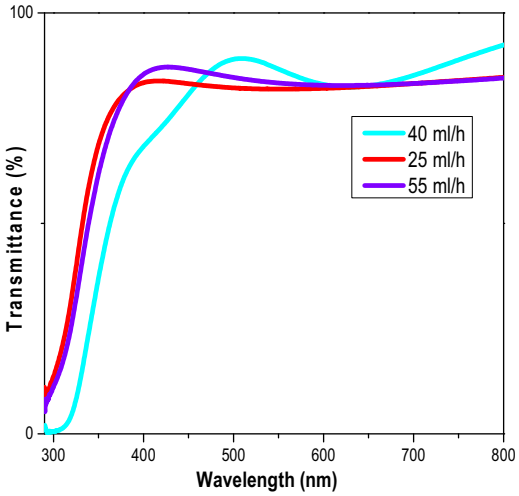

Fig. 6. Optical transmittance spectra of In_2O_3 thin films as a function of flow rate.

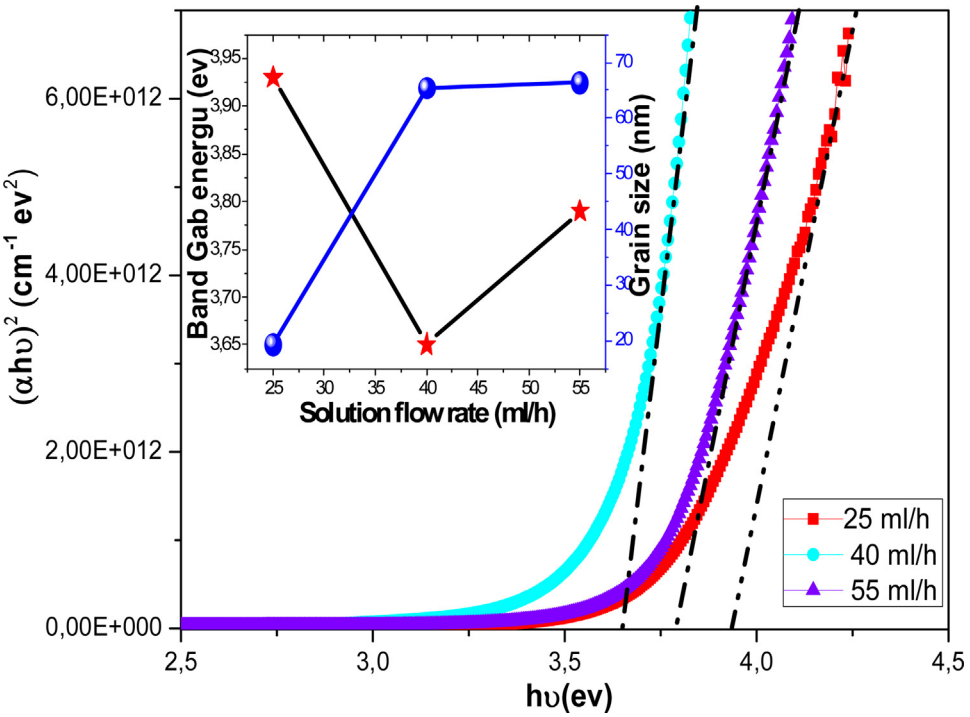

Fig. 7. Optical band gap energy for the In_2O_3 thin films deposited at various flow rate.

The optical band gap of In_2O_3 films is estimated from Tauc relationship [29]

$$(\alpha h\nu)^2 = A(hv - Eg) \quad (4)$$

where α is absorption coefficient, A is the constant independent of photon energy ($h\nu$), h is the Planck constant and Eg is the optical band gap. The variation of band gap Eg as a function of solution flow rate is shown in Fig. 7. The Film deposited at 25 ml/h has higher band gap 3.93 eV, this due to the quantum confinement effect due to the small grain size [30]. It is well known that the absorption edge blue shift with decreasing grain size [31]. The optical gap of films which deposited at 40 ml/h and 55 ml/h is close to its value for In_2O_3 bulk material. However the value of the optical band gab for the film deposited at 55 ml/h (Eg = 3.79 eV) somehow big which is not due to the quantum size confinement, but probably due to the reduction of defects density at the grain boundaries of the film [32]. The obtained energy gap values are in good agreement with other literature reports [30,31,23].

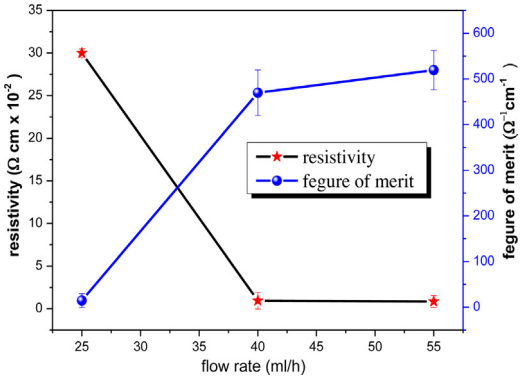

Fig. 8. Electrical resistivity and figure of merit of In_2O_3 thin film deposited at various flow rate.

Table 2
Square resentence of various oxide thin films.

R_S (Ω/□)	thin film	Deposition technique	Deposition temperature (°C)	reference
1.03 10^3				
2.4 10^2				
2 10^2		ultrasonic Spry	350	This work
11 10^3	In_2O_3	Pneumatic spray	350	[37]
0.9 10^3		ultrasonic Spry	400	
1.2 10^2	ITO	reactive thermal evaporation	167	[38]
2 10^1	IMO	spray pyrolysis	400	[11]
138	SnO_2:F	spray ultrasonic	480	[39]
4 10^3	ZnO	spray pyrolysis	450	[40]

Unit of sheet resistance Rs; [□] means square.

The variation of electrical resistivity (ρ) of the In_2O_3 films as a function of the solution spray rate is shown in Fig. 8. It is observed that the resistivity of the films decreases with the increase of the solution spray rate. This can be attributed to the decrease in scattering sites due to the improvement in the film crystallinity [33]. In addition, the oxygen concentrations in the crystal have important impacts on the electronic properties of In_2O_3. We believe that the oxygen concentration in the film deposited at 55 ml/h is lowest due to the increase of deposition rate which lead to prevent the incorporation of the oxygen in the structure [12]. This means the increase of the oxygen vacancies. The latter causes decrease in the electrical resistivity due to the raise of carrier concentrations in this film [34,35]. These values of electrical resistivity characteristic have been attained by other authors [21,36]. On the Other hand, the conductivity studies of the majority of transparent conductive films on glass substrates, such as undoped indium oxide, ITO, ZnO and SnO_2 films are studied by using square resistance which is the edge-to-edge series resistance of any square cut out of the same sheet of TCO film. The results of the Rsq for our films and other conductive TCO thin films are reported in Table 2. On the one hand, these results show that the square resistance depends on film nature, deposition parameters and the used technique. On the other hand, the values of the square resistance obtained in the current study are satisfactory.

Figure of merit for a transparent conductor can be defined By the equation $F = (-\rho \ln T)^{-1}$, where ρ is the electrical resistivity and T is the average transmittance in the wavelength range of 400–800 nm [41]. The figure of merit for the In_2O_3 thin film deposited at 25 ml/h was estimated at 14.71 Ω^{-1} cm^{-1}. However, for the film deposited at t 55 ml/h, the figure of merit increases to 519.35 Ω^{-1} cm^{-1} (see Fig. 8).

4. Conclusions

The effect of the flow rate on the crystalline state, surface morphology, optical, and electrical properties of In_2O_3 films was investigated. X-ray diffraction reveals a polycrystalline nature for all films. Depending on the results of the current study we found that the preferential orientation change with the change of Solution Spray Rate. SEM images show that with the increase of the solution flow rate the films surface are porous, relatively smooth and granular without discernible boundaries.

The optical characterization showed that our films are transparent. And the transmittance of In_2O_3 films increase with the increase of the solution flow rate. We have found also that the optical gap is varied between 3.65 eV and 3.93 eV, and the values found of resistivity are between 30 10^{-2} Ω cm and 8.5 10^{-3} Ω cm. these results indicate that the In_2O_3 film prepared by this technique is a promising candidate for photovoltaic device applications.

References

[1] S.O. Kucheyev, J.S. Williams, C. Jagadish, J. Zou, C. Evans, A.J. Nelson, A.V. Hamza, Phys. Rev. B 67 (09) (2003) 4115.
[2] J. Joseph Prince, S. Ramamurthy, B. Subramanian, M. Jayachandran, Spray pyrolysis growth and material properties of In_2O_3 films, J. Cryst. Growth 240 (2002) 142–151.
[3] Z. Kaiyu, J. Wang, Thin Solid Films 162 (1988) 305.
[4] T.K. Subramanyam, B. Srinivasula Naidu, S. Uthanna, Appl. Surf. Sci. 169–170 (2001) 529.
[5] A.K. Kulkarni, Kirk H. Schulz, T.S. Lim, M. Khan, Thin Solid Films 345 (1999) 273–277.
[6] A. Ayeshamariam, et al., Ceram. Int. 40 (2014) 1321–1328.
[7] V. Marotta, S. Orlando, G.P. Parisi, A. Giardini, G. Perna, A.M. Santoro, V. Capozzi, Electrical and optical characterization of multilayered thin film based on pulsed laser deposition of metal oxides, Appl. Surf. Sci. 168 (2000) 141–145.
[8] A.K. Saxena, S.P. Singh, R. Thangaraj, O.P. Agnihotri, Thin Solid Films 117 (1984) 95.
[9] A. Korotcenkov, V. Brinzari, M. Vasiliev, A. Ivanov, J. Cornet, A. Cabot, J. Arbiol, Sens. Actuators B 99 (2004) 297–303.
[10] A. Bouhdjer, H. SaidiH. Bendjedidi, Y. Benkhetta, I. Bouhaf, J. Semicond. 36 (8) (2015).
[11] S. Parthiban, E. Elangovan, K. Ramamurthi, Solar Energy Mater. Solar Cells 94 (2010) 406–412.
[12] Z. Qiao, R. Latzb, D. Mergela, Thin Solid Films 466 (2004) 250–258.
[13] D.P. Pham, et al., Thin Solid Films 570 (2014) 16–19.
[14] Zhaohui Qiao, Dieter Mergel, Thin Solid Films 484 (2005) 146–153.
[15] P. Thilakan, J. Kumar, Vacuum 48 (1997) 463.
[16] H. Seffes, C. Imawan, F. Solzbacher, E. Obermeir, Reactively rfsputtered In2O3 thin films for the detection of NO2, in: Proceedings of Eurosensors XIII on CD, The Hague, The Netherlands, 12–15 September, 1999, pp. 871–874.
[17] L. I.Maissel, R. Glang, Handbook of Thin Film Technology, New York, McGraw Hill, 1970.
[18] K.L. Chopra, Thin Film Phenomena, McGraw-Hill, New York, 1969, pp. 270.
[19] G.B. Williamson, R.C. Smallman, III. Dislocation densities in some annealed and cold-worked metals from measurements on the X-ray debye-scherrer spectrum, Philos. Magazine 1 (1956) 34–46.
[20] C.M. Mahajan, M.G. Takwale, J. Alloys Compd. 584 (2014) 128–135.
[21] Jin-Hong Lee, Byung-Ok Park, Surf. Coat. Technol. 184 (2004) 102–107.
[22] G. Korotcenkov, V. Brinzari, A. Cerneavschi, A. Cornet, J. Morante, A. Cabot, J. Arbiol, Sens. Actuators B 84 (1) (2002) 37–42.
[23] M. Jothibas, et al., J. Mol. Struct. 1049 (2013) 239–249.
[24] I.Y.Y. Bu, Ceram. Int. 40 (2014) 345–3445.
[25] A. Bendjedidi, H. Attaf, S. Aida, A. Bouhdjar, Y. Benkhetta, J. Semicond. 36 (12) (2015).
[26] D. Beena, K.J. Lethy, R. Vinodkumar, V.P. Mahadevan Pillai, V. Ganesan, D.M. Phase, S.K. Sudheer, Appl. Surf. Sci. 255 (2009) 8334–8342.
[27] N. Lehraki, M.S. Aida, S. Abed, N. Attaf, A. Attaf, M. Poulain, Curr. Appl. Phys. 12 (2012) 1283–1287.
[28] S.A. Studenikin, N. Golego, M. Cocivera, J. Appl. Phys. 83 (1998) 210.
[29] J. Bardeen, F.J. Blatt, L.H. Hall, Proceedings of Atlantic City Photoconductivity Conference in 1954, Wiley and Chapman and Hall, New York, 1956, p. 146.
[30] N.G. Pramod, S.N. Pandey, Ceram. Int. 40 (2014) 3461–3468.
[31] M.A. Majeed Khana, Wasi Khan, Maqusood Ahamed, Mansour Alhoshan, Mater. Lett. 79 (2012) 119–121.
[32] J.D. Dow, D. Redfield, Phys. Rev. B 5 (1972) 594.
[33] R.K. Gupta, K. Ghosh, S.R. Mishra, P.K. Kahol, Appl. Surf. Sci. 254 (2008) 4018–4023.
[34] Kazuhiro Kato, Hideo Omoto, Takao Tomioka, Atsushi Takamatsu, Thin Solid Films 520 (2011) 110–116.
[35] Wen-Fa WuU, Bi-Shiou Chiou, Thin Solid Films 298 (1997) 221–227.
[36] C.-C. Yu, et al., Vacuum 102 (2014) 63–66.
[37] M. Girtan, et al., Thin Solid Films 427 (2003) 406–410.
[38] A. Amaral, et al., Surf. Coat. Technol. 125 (2000) 151–156.
[39] B. Benhaoua, et al., Superlattices Microstruct. 83 (2015) 78–88.
[40] T. Prasada Rao, M.C. Santhoshkumar, Appl. Surf. Sci. 255 (2009) 7212–7215.
[41] V. Senthilkumar, P. Vickraman, Curr. Appl. Phys. 10 (2010) 880.